Magnetic properties of the $Fe_xMn_{0.600-x}Al_{0.400}$, $0.200 \leq x \leq 0.600$, disordered alloy series

2002 J. Phys.: Condens. Matter 14 6531

(http://iopscience.iop.org/0953-8984/14/25/320)

INSTITUTE OF PHYSICS PUBLISHING JOURNAL OF PHYSICS: CONDENSED MATTER

J. Phys.: Condens. Matter **14** (2002) 6531–6542 PII: S0953-8984(02)32995-3

Magnetic properties of the $Fe_xMn_{0.600-x}Al_{0.400}$, $0.200 \leqslant x \leqslant 0.600$, disordered alloy series

Claudia González[1,2], German A Pérez Alcázar[1], Ligia E Zamora[1], Jesus A Tabares[1] and Jean-Marc Greneche[2]

[1] Departamento de Física, Universidad del Valle, AA 25360, Cali, Colombia
[2] Laboratoire de Physique de L'Etat Condensé, UMR CNRS 6087, Université du Maine, 72085 Le Mans, Cedex 9, France

Received 24 January 2002, in final form 23 April 2002
Published 14 June 2002
Online at stacks.iop.org/JPhysCM/14/6531

Abstract

The magnetic properties of the $Fe_xMn_{0.600-x}Al_{0.400}$ ($0.200 \leqslant x \leqslant 0.600$) disordered alloys were investigated by means of Mössbauer spectrometry, ac magnetic susceptibility, and ac calorimetry measurements. Our results are summarized in a magnetic phase diagram, which includes an antiferromagnetic phase for $x \leqslant 0.300$ at $T \leqslant 225$ K, a ferromagnetic one for $x \geqslant 0.425$ at $T \leqslant 340$ K, and a paramagnetic phase for high temperatures and all the compositions. This phase diagram also shows for the first time both a re-entrant spin-glass–ferromagnetic transition line for $x \geqslant 0.425$ and $T \leqslant 60$ K and a re-entrant spin-glass–antiferromagnetic one for $x \leqslant 0.300$ and $T \leqslant 40$ K. The occurrence of superparamagnetic-like blocked events (for $0.300 \leqslant x \leqslant 0.600$ and at $T \approx 200$ K) is associated with the presence of Fe-rich magnetic clusters which can originate from the disordered atomic character of the alloys.

(Some figures in this article are in colour only in the electronic version)

1. Introduction

Disordered alloys in the Fe–Mn–Al system are of great interest from both the theoretical and experimental points of view. Indeed, they can be considered as excellent candidate materials for showing spin-glass (SG) and re-entrant spin-glass (RSG) behaviour, as a consequence of the presence of competing ferromagnetic (F) and antiferromagnetic (AF) interactions: the Fe–Fe and Fe–Mn interactions, respectively. Let us recall that the SG state results from magnetic disorder and magnetic frustration, while the RSG state is due to frustrated spins within a magnetic matrix that can be either ferromagnetic or antiferromagnetic. Pérez Alcázar *et al* [1] showed that, at room temperature (RT), the Fe–Mn–Al system evolved, in the bcc phase, from a ferromagnetic to a paramagnetic phase when either the Al or the Mn concentration was increased. This evolution was proved to occur by Mohan Babu and Bansal [2] for the pseudo-binary alloy system $Fe_{75-x}Mn_xAl_{0.25}$. A theoretical calculation by Rosales Rivera

et al [3], using Bogoliubov's inequality method [4] and the mean-field renormalization-group (MFRG) method [5] applied to a diluted and random-bond Ising model, permitted interpretation of the previously found ferromagnetic-to-paramagnetic (P) evolution and led, for the first time in the literature as far as we are aware, to it being postulated that both SG and RSG phases occur in this system. In addition to this theoretical scenario, it was postulated by Zamora *et al* [6] that the AF phase could appear in the Fe–Mn–Al system for high Mn content, the F phase for high Fe content, the SG as the low-temperature phase for intermediate Fe and Mn contents, and the RSG as the low-temperature phase for high Fe or Mn contents. The presence of P and SG phases in the $Fe_{0.5}(Mn_xAl_{1-x})$ with $0 < x < 1$ series was demonstrated experimentally by Kobeissi [7]. Experimental evidence of RSG phenomenology in this system was reported by Pérez Alcázar and co-workers [8], obtained by studying the $Fe_{0.45}Mn_{0.30}Al_{0.25}$ alloy using Mössbauer and magnetization techniques. A study of $Fe_{0.89-x}Mn_{0.11}Al_x$ alloys [9] revealed that: (1) the RSG transition temperature occurs at $T = 50$ K for $x = 0.4$; and (2) this transition temperature strongly depends on the Al concentration. Recently, Zamora *et al* [10] proposed an experimental magnetic phase diagram for the $Fe_xMn_{0.7-x}Al_{0.3}$ ($0.40 \leqslant x \leqslant 0.58$) alloy series obtained by means of Mössbauer spectrometry and ac magnetic susceptibility. This phase diagram, which includes the P, F, and RSG–F phases, was adequately reproduced by a diluted and random-bond Ising model on the basis of the MFRG method. More recently, an experimental magnetic phase diagram was also proposed for the $Fe_xMn_{0.3}Al_{0.7-x}$ ($0.275 \leqslant x \leqslant 0.525$) alloy system [11]. As in the previous work, this phase diagram includes the P, F, and RSG–F, phases but in this case the AF and RSG–AF phases were obtained for $x \leqslant 0.375$. For this concentration range and at temperatures above those for which the AF phase is observed, the occurrence of superparamagnetic-like blocked events was reported.

In 1996 the present authors reported [12] preliminary work on some alloys of the system $Fe_xMn_{0.6-x}Al_{0.4}$ and reported the occurrence of a RSG–AF transition for $0.2 \leqslant x \leqslant 0.35$, a RSG–F transition for high Fe contents, a pure SG transition for $0.35 \leqslant x \leqslant 0.5$, and superparamagnetic (SPM) blocking behaviour above the pure SG region and below 175 K. This was the first time that SPM behaviour was reported in the Fe–Mn–Al system.

The aim of the present work is to elucidate, on the basis of ^{57}Fe Mössbauer spectrometry, ac magnetic susceptibility, and ac calorimetry measurements, the possible occurrences of SG, RSG, and SPM behaviours in the $Fe_xMn_{0.600-x}Al_{0.400}$, $0.200 \leqslant x \leqslant 0.600$, disordered alloys. Mössbauer spectrometry is a suitable technique, which provides relevant information due to its atomic-scale probe, while its time measurement (typically $\sim 6 \times 10^{-8}$ s for a ^{57}Fe probe nucleus) makes it complementary to static and ac magnetic measurements in investigating dynamic effects, i.e. in estimating the magnetic blocking temperatures.

2. Experimental techniques

The samples were prepared by melting high-purity Fe, Al, and Mn powders in an arc furnace and under an argon atmosphere. The melted materials were kept at 1000 °C for one week in evacuated quartz tubes and subsequently quenched in ice-water. Powder prepared by crushing the quenched buttons was used for the x-ray diffraction and ^{57}Fe Mössbauer spectrometry. X-ray diffraction measurements showed that all the alloys are in the bcc phase. Transmission Mössbauer spectra were recorded at room temperature for all the samples and at temperatures between 4.2 and 320 K for the $x = 0.500$ sample using a constant-acceleration spectrometer with a ^{57}Co/Rh source and a bath cryostat. The spectra were fitted using the MOSFIT program [13] including a discrete hyperfine-field distribution and, in most cases, additional paramagnetic components. The values of the isomer shift are referred to that of natural Fe.

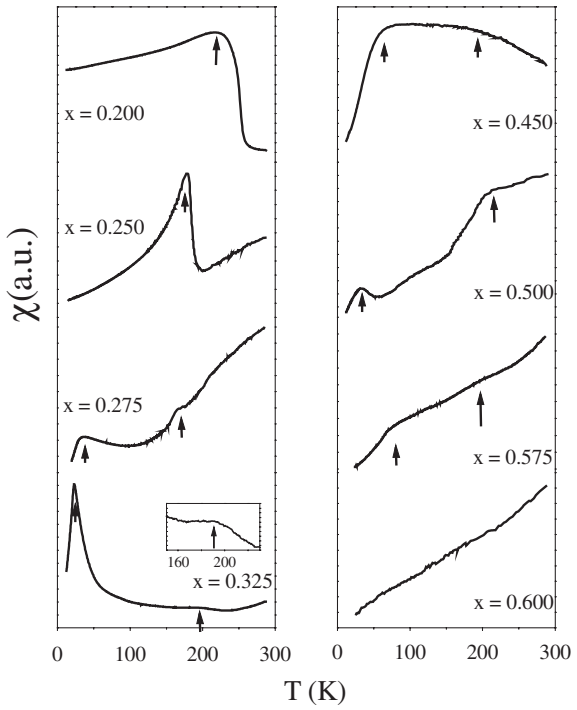

Figure 1. Ac susceptibility versus temperature measurements for some samples at $f = 175$ Hz.

The ac susceptibility measurements were carried out on cylindrical pressed powder samples, 3 mm in diameter and 3–4 mm in height, under an ac field of amplitude 3×10^{-4} T and a biasing dc field of 0.001 T, and at a frequency of 175 Hz. In some cases, the dependences of the susceptibility on the applied dc field (0–0.002 T) and frequency (40–3000 Hz) were also studied. The ac calorimetry measurements were carried out on sheets (1 mm ^{2}–170 μm thick) using a calorimeter with a helium closed-cycle cryogenerator at temperatures ranging from 12 up to 295 K.

3. Experimental results and discussion

3.1. Ac magnetic susceptibility measurements

The temperature dependences of the ac susceptibility were obtained for the samples covering the whole compositional range studied, from $x = 0.200$ to 0.600. Figure 1 shows some of them. The curves exhibit either well defined peaks or some less pronounced ones. These peaks, indicated by arrows in figure 1, are associated with critical temperatures. In the case of less pronounced peaks, each critical temperature is defined as corresponding to the intersection of the lines extrapolating the temperature dependences of the susceptibility on either side of the peak. In figure 1 one notes that the ac curves for the $x = 0.200$, 0.225, and 0.250 samples show a peak located at 220, 200 and 180 K, respectively, which can be associated with an AF-to-P transition for such compositions, according to the results listed in [3, 6]. This transition temperature decreases when x increases. For $x = 0.275$ a new peak appears for low temperature and it always appears for other concentrations ($0.275 \leqslant x \leqslant 0.575$) in the range 25–60 K. According to [3, 6], these peaks can be attributed to SG or RSG phase

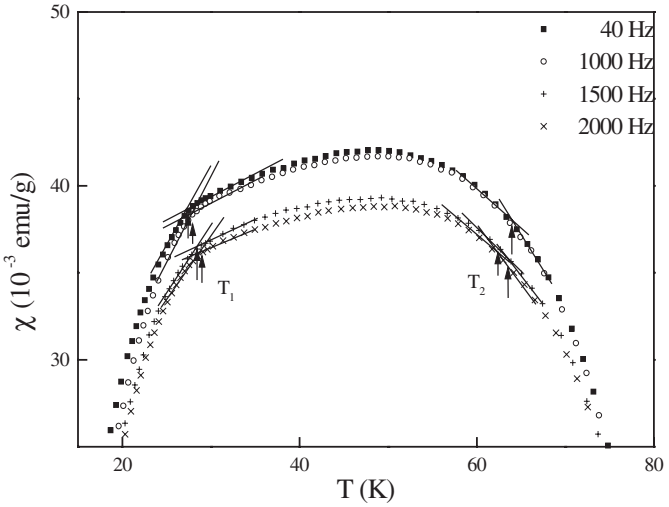

Figure 2. Ac susceptibility for the $x = 0.300$ sample measured at dc field of 0.001 T and four different frequencies.

transition. The peak associated with the AF phase also appears in the $x = 0.275$ and 0.300 samples at 160 and 60 K, respectively, showing that the stability of the AF phase decreases when x increases (less Mn content). For the $x = 0.300$ sample a new peak appears near 175 K, that is always present up to $x = 0.575$ in the range 175–210 K. These new peaks are not so well resolved as those obtained for the SG and AF transitions, but as will be shown they appear clearly in the ac calorimetry measurements. These transitions might correspond to a superparamagnetic blocking temperature associated with large Fe-rich clusters as recently proposed [11], on the basis of low-field and high-field magnetization measurements on the $Fe_{0.275}Mn_{0.300}Al_{0.425}$ sample.

The AF character which was proposed for samples with $x = 0.200$, 0.225, and 0.250 was confirmed by both the frequency and dc field dependences of the ac magnetic susceptibility measurements. The peaks detected in the ac magnetic susceptibility versus temperature curves for these samples show positions and intensities which change in a random way with the increase of the frequency and the dc field, respectively. Such behaviour is associated with an AF transition, according to the literature [14].

In order to prove the existence of the postulated SG and RSG transitions, we measured both the frequency and dc field dependences of the low-temperature peak in the ac magnetic susceptibility curves for some of the samples with a composition range $0.275 \leqslant x \leqslant 0.575$. The associated transition temperature shifts to high values and decreases in intensity when the frequency increases, while the susceptibility peak becomes less pronounced when the dc field increases. These two features are typical of a SG behaviour [10, 15]. One concludes that this peak corresponds to a RSG–AF-type transition, remembering that this sample exhibits another peak at $\sim$160 K attributed to an AF transition. The most typical RSG transition [16] was detected for the $x = 0.300$ sample. To prove this, we obtained for this sample different ac susceptibility versus temperature curves at different frequencies. The results are shown in figure 2, in which it can be noted how this curve is affected by the frequency. The change of curvature at low temperature (T_1) is shifted to high temperature as the frequency increases, while that at high temperature (T_2) changes its position in a random way when the frequency increases. These behaviours permit one to conclude that T_1 corresponds to a SG transition [7]

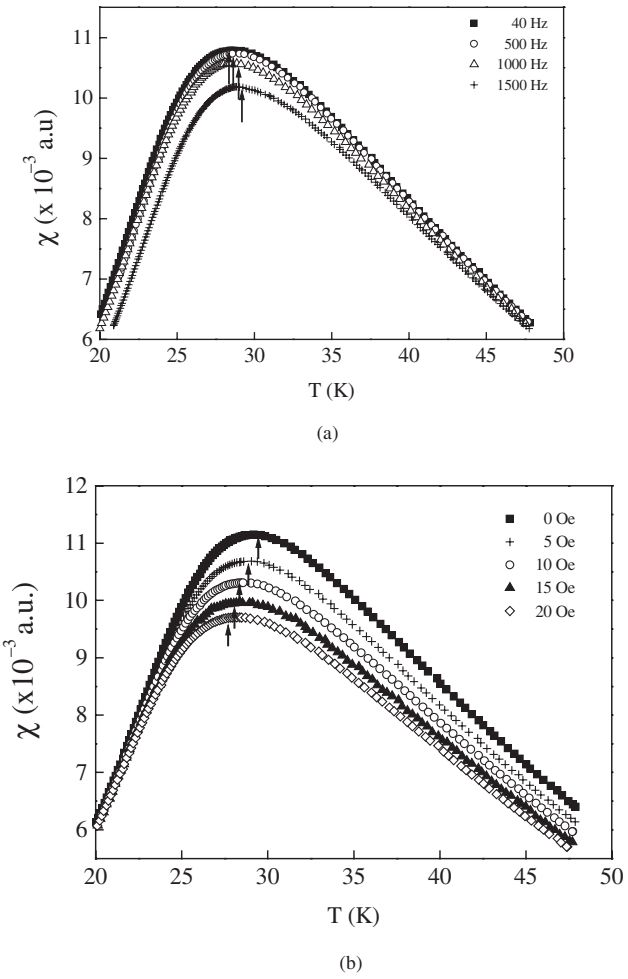

Figure 3. Ac susceptibility versus temperature for the $x = 0.375$ sample. (a) Frequency and (b) dc field dependences.

while T_2 is associated with an AF transition [14]. As can be noted in figure 2, these critical temperatures were each obtained as corresponding to the intersection of the lines extrapolating the temperature dependence of the susceptibility on either side of each of the peaks. Very similar results were obtained for the samples with the composition range $0.425 \leqslant x \leqslant 0.575$; indeed, the low-temperature peak observed in figure 1 between 25 and 60 K, for these samples, corresponds to a RSG–F transition. Details of the frequency dependence of the ac susceptibility versus T for the lower-T peak of the sample with $x = 0.500$ were reported in [17], in order to prove the SG character of this transition.

Figures 3(a) and (b) show both the frequency and the dc field dependences of the ac magnetic susceptibility for the sample with $x = 0.375$ near the low-temperature peak detected for this sample. Such a behaviour, typical of a SG transition, is also evidenced for $x = 0.325$, 0.350, and 0.400. It is important to emphasize that these alloy samples correspond to intermediate Fe and Mn contents, that compositional region in which all the ferromagnetic and antiferromagnetic interactions present competing behaviour. The theoretical predictions

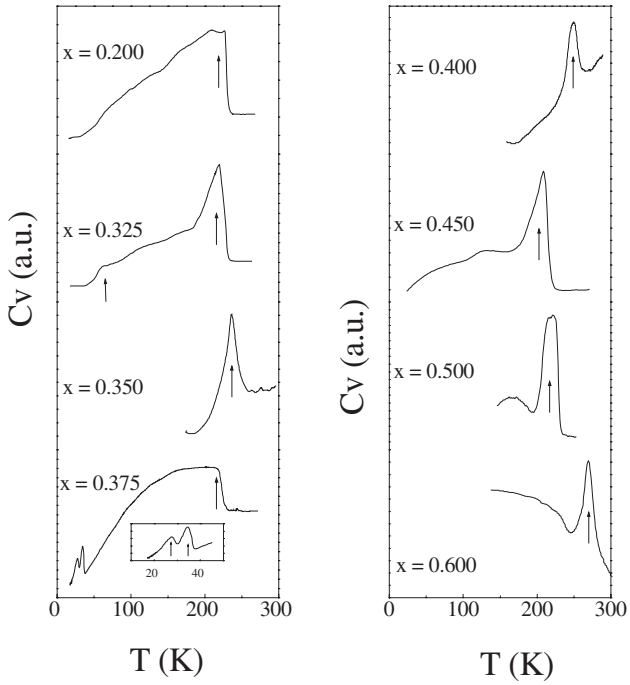

Figure 4. Specific heat versus temperature curves for some samples.

of Rosales Rivera *et al* [3] and Zamora *et al* [6] in conjunction with the presence of well defined peaks obtained for the ac susceptibility curves for these samples, allow a pure SG transition for the composition region $0.325 < x < 0.400$ to be proposed.

Finally, and concerning the ac susceptibility curves shown in figure 1, peaks that are not well defined can also be observed at $T \approx 170$ and 215 K for $x = 0.450$ and 0.550, respectively. Similar peaks were obtained in the ac susceptibility curves at $T \approx 180$, 210, 200, and 180 K for $x = 0.425$, 0.500, 0.525, and 0.575, respectively. These peaks are also attributed to the occurrence of superparamagnetic-like blocking events. In this case, as will be detailed later, these events occur in a ferromagnetic matrix.

3.2. Ac calorimetry measurements

Figure 4 shows the specific heat versus temperature curves, obtained by ac calorimetry measurements for some of the alloys studied. For low x-values (low Fe contents), the result which corresponds to $x = 0.200$ presents an anomaly at $T \approx 225$ K only. This temperature is found close to that detected by ac magnetic susceptibility measurements, confirming the postulated pure AF transition. Similar results were obtained for the $x = 0.325$, 0.350, 0.375, 0.400, 0.450, 0.475, 0.500, and 0.600 samples, for which well defined peaks were registered at $T \approx 220$, 235, 218, 250, 205, 217, 222, and 251 K, respectively. As pointed out before, less intensive peaks were obtained for the same samples with ac magnetic susceptibilities within the range 200–210 K. This can be associated with SPM blocking temperatures according to the experimental facts demonstrated in [11]. In general, the curves of specific heat versus temperature do not show at low temperature additional peaks which could be associated with a SG transition, except for the $x = 0.325$ and 0.375 samples for which a peak is present. As was

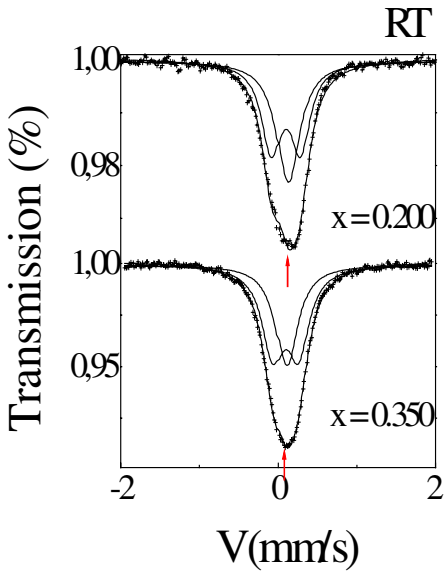

Figure 5. Mössbauer spectra at RT for the samples with $x = 0.200$ and 0.350.

pointed in many references (see for example [15]), the specific heat versus T curves for SG systems present very broad peaks near the freezing temperature obtained from ac susceptibility. However, in our case, low-temperature peaks do not appear, because specific heat measurement is not a suitable route to determining SG transition temperatures.

3.3. ^{57}Fe Mössbauer spectrometry

Figure 5 presents the Mössbauer spectra at RT for the alloys with compositions 0.200 and 0.350. The RT spectra exhibit quadrupolar hyperfine structures consistent with paramagnetic states of these alloys. The spectra were fitted in two ways: one using a single line and a doublet and the other using a single line and a quadrupolar distribution in order to describe the disordered character of the samples. These two methods give very good fits, but the second one gives a very narrow quadrupolar distribution which can be assumed to be only one doublet. Thus we adopt the first fitting method. Mössbauer spectra at RT for the alloys with compositions 0.250, 0.300, and 0.400 are very similar to those shown in figure 2.

A higher Fe content ($0.450 \leqslant x \leqslant 0.600$) favours the progressive development of a magnetic hyperfine structure, as is illustrated in figure 6. All the spectra were fitted with a hyperfine-field distribution (HFD), and a quadrupolar and a single-line component. The mean-field value for these ferromagnetic samples increases with the Fe concentration. The increase with the Fe content of the ferromagnetic character can also be noted in the HFD. In these samples, the low-field Fe sites are more probable for low x-values, while for large x-values the more probable Fe sites are those with high fields. One could suggest that the single-line component and the quadrupolar doublet correspond to paramagnetic sites surrounded by symmetric and non-symmetric charge distribution, respectively.

It is important to emphasize that the mean isomer shift (δ) for all the samples decreases when the Fe concentration (x) increases, i.e. the substitution of Fe atoms for Mn atoms increases. The increment of the Fe content brings about a decrease in the electron population

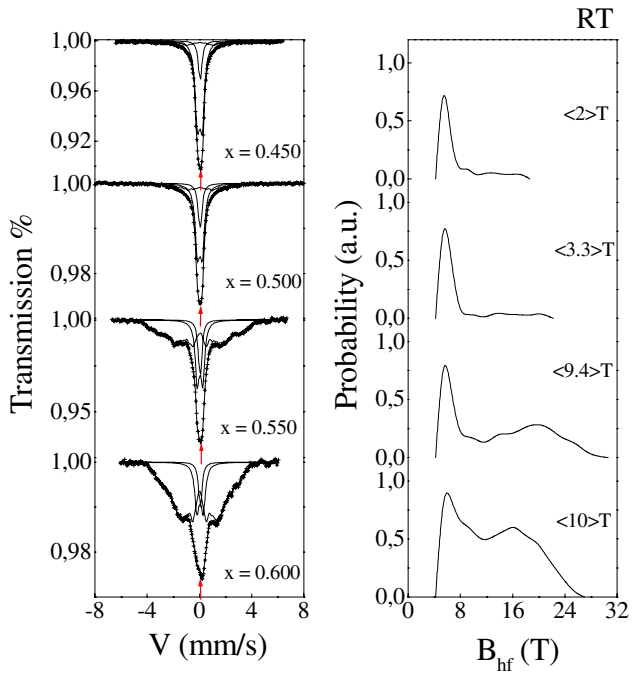

Figure 6. Mössbauer spectra and their corresponding hyperfine-field distributions for the samples with $0.450 \leqslant x \leqslant 0.600$ at RT.

of the conduction band and then a decrease in the 3d electron density around the Fe nucleus. If the electron density of the 3d shell of Fe is reduced, the shielding of the s electron at the nucleus is reduced; therefore, the s electron density increases and, consequently, the isomer shift decreases. This change of δ is indicated by arrows in figures 5 and 6.

Figure 7 shows the Mössbauer spectra of samples in the $0.200 \leqslant x \leqslant 0.500$ composition range recorded at 4.2 K. In this case the samples were fitted with a singlet, a doublet, and a HFD. At this temperature, the samples with x up to 0.400, which at RT are P, present now magnetic structure with low magnetic hyperfine fields, whereas for the sample with $x = 0.500$, which is F at RT with low mean hyperfine fields, now presents larger hyperfine fields. According to previous results [11], such a description is *a priori* consistent with the AF character of the sample with $x = 0.200$, the SG character of the samples with $x = 0.300$, 0.350, and 0.400, and the RSG character of the $x = 0.500$ sample, detected by ac measurements.

As was postulated on the basis of the ac magnetic susceptibility and ac calorimetry, in the composition region between $x = 0.425$ and 0.575 there can be detected some magnetic phases: RSG character in the F phase; re-entrant superparamagnetism (RSPM) character in the F phase; F character in the P phase. In order to prove in a more conclusive way the presence of these phases, Mössbauer spectra were taken at different temperatures for the $x = 0.50$ alloy. These spectra and their corresponding HFD are shown in figure 8 for some temperatures. The spectra for temperatures lower than 330 K were fitted with a single line, a doublet, and a HFD, and that for 340 K with a doublet and a single line. In this case the alloy is ferromagnetic for $T_C < 340$ K and paramagnetic for $\geqslant$340 K. In figure 9 the mean hyperfine field obtained, $\langle B_{\rm hf}\rangle$, is plotted versus temperature. One can observe three kinks in this B_{hf}-curve: one at nearly 30 K, another at 210 K, and the last one at 340 K. The first kink is attributed to the

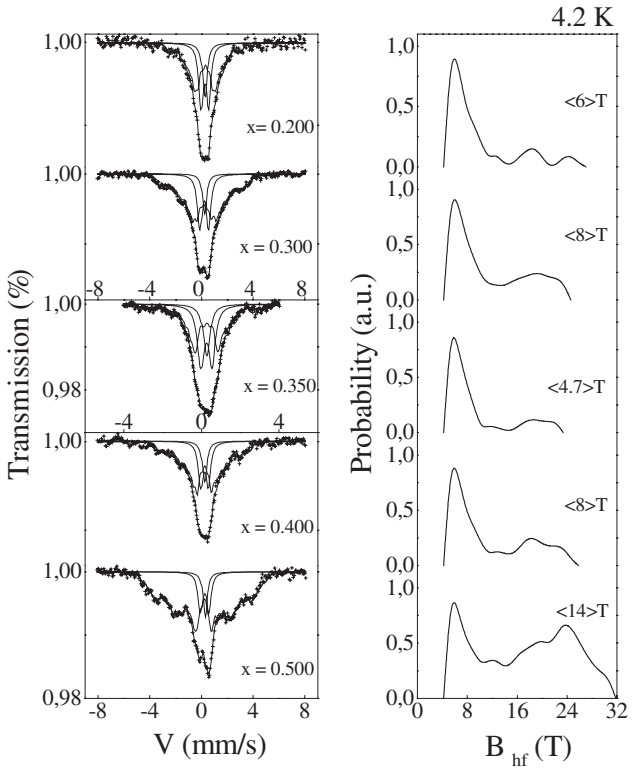

Figure 7. Mössbauer spectra at 4.2 K for the concentrations $x = 0.200$, 0.300, 0.350, 0.400, and 0.500 and their corresponding hyperfine-field distributions.

RSG–F transition, at temperature T_k, in agreement with the ac magnetic susceptibility results; the second one is assigned to the RSPM–F transition, at T_B, in agreement with the ac magnetic susceptibility and the ac calorimetry results; while the last one corresponds to the F–P transition or Curie point of the alloy, at T_C.

The shape of the curve for $\langle B_{\rm hf}\rangle$ shown in figure 9 can be understood remembering that the alloys are disordered and with atoms which behave in ferromagnetic (Fe), antiferromagnetic (Mn), and dilutor (Al) fashion. This disorder and the magnetic behaviour of the atoms permit there to be different magnetic orders: AF for high Mn content; F for high Fe content; SG for intermediate compositions; RSG for low temperatures and below the AF or F phases; and SPM clusters when sites rich in Fe and Mn are very near and isolated by sites of Fe and Mn rich in Al. With this in mind the shape of the $B_{\rm hf}$-curve can be explained on the basis of the following model. At high temperature the alloy is paramagnetic and, at T_C, some spins start becoming parallel due to the existence of ferromagnetic exchange interactions; their number increases as temperature decreases. Due to structural disorder, magnetic dilution, and competitive interactions, some spins (i.e., those being highly frustrated) would remain, however, in the paramagnetic state below T_C. Also, due to the structural disorder, magnetic dilution, and the higher Fe and Al contents, 50 and 40 at.%, respectively, it is possible to have Fe-rich magnetic clusters surrounded by Al atoms. As the temperature decreases, the mean field increases and the clusters are blocked at T_B with a strong tendency to become aligned with the internal field created by the ferromagnetic matrix, giving an extra contribution to the

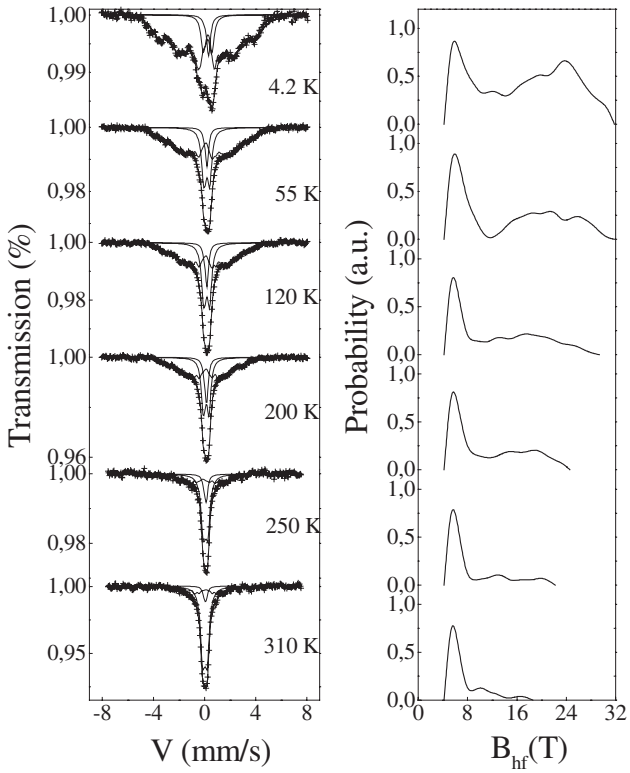

Figure 8. Mössbauer spectra recorded at different temperatures for the $x = 0.500$ sample and their corresponding hyperfine-field distributions.

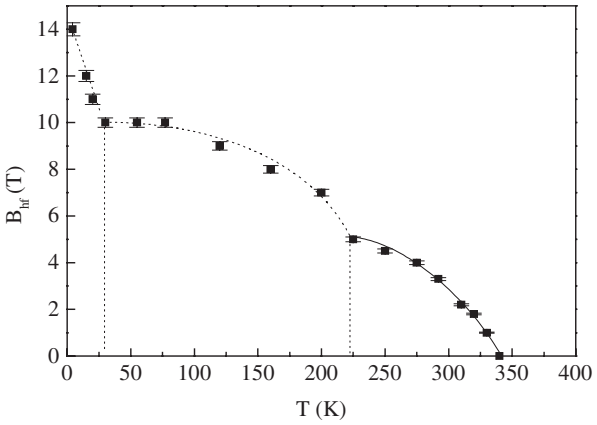

Figure 9. Variation of the mean average hyperfine field versus temperature for the $x = 0.500$ sample.

observed average hyperfine field (the kink at 210 K). At T_k, the spins, which are frustrated due to competitive interactions, will freeze nearly along the internal field direction of the matrix and give in this way the extra contribution observed at 30 K and below.

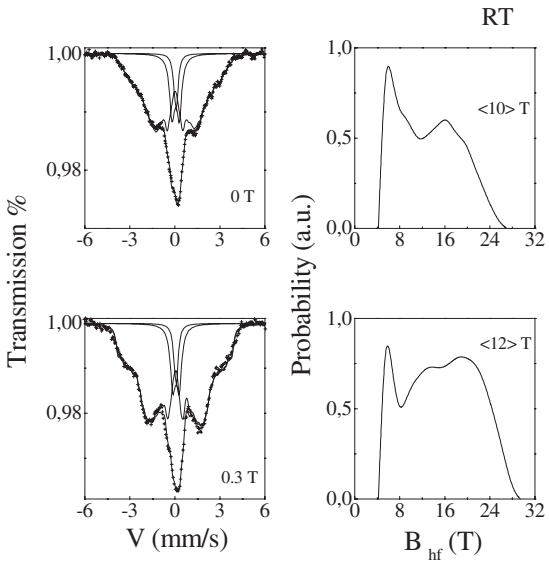

Figure 10. Mössbauer spectra and their corresponding hyperfine-field distributions for the $x = 0.550$ sample (top) without a field and (bottom) with an external field (0.3 T). The mean hyperfine field is given besides the corresponding hyperfine field distribution.

In-field Mössbauer were spectra were recorded to check the magnetic arrangement from the intensities of intermediate lines and the presence of superparamagnetic effects from the evolution of the distribution of hyperfine fields. The external field was applied perpendicular to the direction of the γ-beam. An example is presented in figure 9: we show the Mössbauer spectra of the $x = 0.600$ sample at RT without a field and with a 0.3 T applied field, and their respective HFDs. The significant increases in the intensities of the intermediate lines clearly proves the ferromagnetic character of the sample. For low Fe content, the quadrupolar hyperfine structure remains unchanged in the presence of an external field. At 77 K, in the case of $x = 0.500$, the mean HF increases and the shape of the HFD changes with the applied field. Such features suggest the presence of superparamagnetic effects, contrary to the case for $x = 0.300$, where no changes occur in the presence of an external field.

Taking, together the ac magnetic susceptibility, the ac calorimetry and the Mössbauer data into account permits the magnetic phase diagram to be established. It is presented as figure 11. According to these data, a SG region is observed throughout the composition range between $x = 0.275$ and 0.575 at temperatures below 55 K; an AF region is observed above the SG one and below 225 K in the Fe-poor region—the SG region in this case is of RSG–AF (re-entrant spin-glass–antiferromagnetic) type. A SPM region above the SG region and below 200 K is present for intermediate Fe contents. In this case the SPM clusters appear surrounded by a paramagnetic matrix. Also a SPM region above the SG region and below 240 K is present for high Fe contents. In this case the SG region is of the RSG–F (re-entrant spin-glass–ferromagnetic) type and the SPM region is of the RSPM–F (re-entrant superparamagnetic–ferromagnetic) type. Finally, a ferromagnetic phase for high Fe contents ($0.420 \leqslant x \leqslant 0.600$) and below 340 K occurs. In this case, inside the ferromagnetic matrix there appear some frustrated spins giving rise to the RSG phase and SPM clusters giving rise to the RSPM phase. A paramagnetic region is present for the entire composition region at high temperatures, corresponding to the behaviour for high temperatures in these alloys.

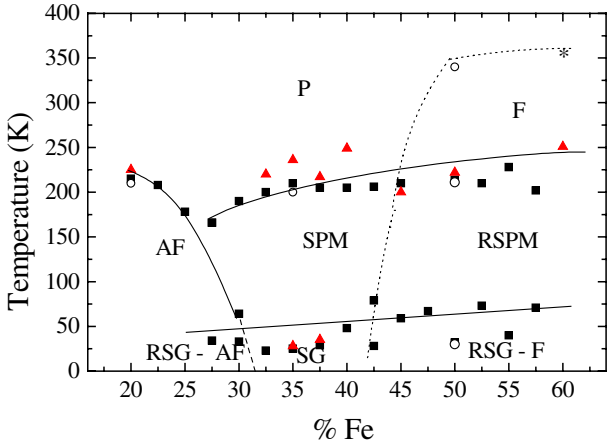

Figure 11. The proposed magnetic phase diagram for the 40 at.% Al alloy series. Full squares, triangles, and open circles correspond to the ac susceptibility data, the calorimetry measurements, and Mössbauer spectrometry data, respectively. The point marked by an asterisk was also obtained by Mössbauer spectrometry and reported in [1].

Acknowledgments

The authors are grateful to the Universidad del Valle, and Colciencias, Colombian Agency, for financial support, as well as Alvaro García for help. One of the authors (Claudia González) would like to thank the Laboratoire de Physique de l'Etat Condensé, Université du Maine, for a research stay. The present work was supported by the ECOS-Nord Colombian–French exchange programme under contract CF99P04.

References

[1] Pérez Alcázar G A, Plascak J A and Galvão da Silva E 1988 *Phys. Rev.* B **38** 2816
[2] Mohan Babu T V S M and Bansal C 1996 *Phys. Status Solidi* b **193** 167
[3] Rosales Rivera A, Pérez Alcázar G A and Plascak J A 1990 *Phys. Rev.* B **41** 4774
[4] Ferreira L G, Salinas S R and Oliveira M J 1977 *Phys. Status Solidi* b **83** 229
[5] Indekeu J O, Maritan A and Stella J L 1982 *J. Phys. A: Math. Gen.* **15** L291
[6] Zamora L E, Pérez Alcázar G A, Bohórquez A, Rosales Rivera A and Plascak J A 1995 *Phys. Rev.* B **51** 9329
[7] Kobeissi M A 1991 *J. Phys.: Condens. Matter* **3** 4983
[8] Zamora L E, Pérez Alcázar G A, Bohórquez A and Tabares J A 1994 *J. Magn. Magn. Mater.* **137** 339
[9] Bremers H, Jarms Ch, Hesse J, Chajwasiliou S, Efthiadis K G and Tsonkalas Y 1995 *J. Magn. Magn. Mater.* **140** 63
[10] Zamora L E, Pérez Alcázar G A, Bohórquez A, Marco J F and González J M 1997 *J. Appl. Phys.* **82** 6165
[11] Zamora L E, Pérez Alcázar G A, Tabares J A, Bohórquez A, Marco J F and González J M 2000 *J. Phys.: Condens. Matter* **12** 611
[12] Pérez Alcázar G A, Zamora L E, Bohórquez A, González E and González J M 1996 *J. Appl. Phys.* **79** 6155
[13] Varret F and Teillet J *MOSFIT Program* (unpublished)
[14] Mulder C A M, Van Duynveldt A J and Mydosh J A 1981 *Phys. Rev.* B **23** 1384
[15] Canella V and Mydosh J A 1972 *Phys. Rev.* B **6** 4220
[16] Mirabeau I, Itoh S, Mitsuda S, Watanabe T, Endoh Y, Hennion M and Papoular R 1990 *Phys. Rev.* B **41** 11 405
[17] González C, Tabares J A, Zamora L E, García A and Pérez Alcázar G A 1998 *Hyperfine Interact.* C **4** 77